PDE1C deficiency antagonizes pathological cardiac remodeling and dysfunction

Walter E. Knight[a,b], Si Chen[a,b], Yishuai Zhang[a], Masayoshi Oikawa[a], Meiping Wu[a,c], Qian Zhou[a], Clint L. Miller[a], Yujun Cai[a], Deanne M. Mickelsen[a], Christine Moravec[d], Eric M. Small[a], Junichi Abe[a], and Chen Yan[a,1]

[a]Aab Cardiovascular Research Institute, Department of Medicine, University of Rochester School of Medicine and Dentistry, Rochester, NY 14641; [b]Department of Pharmacology and Physiology, University of Rochester School of Medicine and Dentistry, Rochester, NY 14641; [c]Department of Cardiology, Shanghai Municipal Hospital of Traditional Chinese Medicine, Shanghai University of Traditional Chinese Medicine, Shanghai, China 201203; and [d]Department of Cardiovascular Medicine, Cleveland Clinic, Cleveland, OH 44195

Cyclic nucleotide phosphodiesterase 1C (PDE1C) represents a major phosphodiesterase activity in human myocardium, but its function in the heart remains unknown. Using genetic and pharmacological approaches, we studied the expression, regulation, function, and underlying mechanisms of PDE1C in the pathogenesis of cardiac remodeling and dysfunction. PDE1C expression is up-regulated in mouse and human failing hearts and is highly expressed in cardiac myocytes but not in fibroblasts. In adult mouse cardiac myocytes, PDE1C deficiency or inhibition attenuated myocyte death and apoptosis, which was largely dependent on cyclic AMP/PKA and PI3K/AKT signaling. PDE1C deficiency also attenuated cardiac myocyte hypertrophy in a PKA-dependent manner. Conditioned medium taken from PDE1C-deficient cardiac myocytes attenuated TGF-β–stimulated cardiac fibroblast activation through a mechanism involving the crosstalk between cardiac myocytes and fibroblasts. In vivo, cardiac remodeling and dysfunction induced by transverse aortic constriction, including myocardial hypertrophy, apoptosis, cardiac fibrosis, and loss of contractile function, were significantly attenuated in PDE1C-knockout mice relative to wild-type mice. These results indicate that PDE1C activation plays a causative role in pathological cardiac remodeling and dysfunction. Given the continued development of highly specific PDE1 inhibitors and the high expression level of PDE1C in the human heart, our findings could have considerable therapeutic significance.

cyclic nucleotide | phosphodiesterase | cardiac remodeling | heart failure

Heart failure, the inability of the heart to provide sufficient blood to the body, remains one of the leading global causes of death (1). Pathological cardiac remodeling plays a pivotal role in the development of heart failure and is characterized by myocyte hypertrophy and death, fibroblast activation, and extracellular matrix deposition, ultimately leading to functional defects (2). Therefore, identifying novel molecular regulators underlying the pathogenesis of cardiac remodeling is essential for the continued development of therapeutic agents. In the heart, the second messengers cyclic AMP (cAMP) and cyclic GMP (cGMP) are implicated in numerous signaling pathways, from short-term regulation of myocyte contraction/relaxation to long-term functions in growth and survival. In cardiac cells there are multiple functionally distinct pools of cyclic nucleotides. Acutely, activation of β-adrenergic receptor (β-AR) cAMP signaling is procontractile, whereas chronic β_1-AR activation elicits detrimental prohypertrophic (2) and proapoptotic effects (3, 4). By contrast, adenosine-derived cAMP signaling can attenuate many of these effects (5). Moreover, cAMP produced by different adenylyl cyclases (ACs) has different cardiac effects: AC5-derived cAMP is detrimental, whereas AC6-derived cAMP is protective in pathological cardiac remodeling (6). cGMP is generated from both the soluble and particulate guanylyl cyclases (GCs), and many studies have shown negative inotropic and cardioprotective effects (7, 8) from cardiac cGMP signaling. Together, these lines of evidence indicate that different cyclic nucleotide signaling modules have distinct, unique, and often even opposing physiological roles.

Cyclic nucleotide phosphodiesterases (PDEs), by catalyzing cyclic nucleotide hydrolysis, play a critical role in regulating the amplitude, duration, and compartmentalization of cyclic nucleotide signaling. PDEs constitute a superfamily of enzymes with 22 different genes and more than 100 mRNAs grouped into 11 broad families (PDE1–PDE11) based on distinct structural, kinetic, regulatory, and inhibitory properties. It has become increasingly clear that cyclic nucleotide degradation by PDEs is not a constitutive process but rather is differentially regulated in response to varying physiological and pathological circumstances. PDEs play diverse roles in cardiac dysfunction: Chronic inhibition or reduced expression of PDE3A (4) and PDE4D (9) worsens the development of cardiac dysfunction, whereas the inhibition of PDE5 (10) and PDE9 (11) protects against it. PDE1 represents a major PDE activity in human myocardium (12), but its role in cardiac biology and disease remains elusive. Three distinct genes, *PDE1A*, *-1B*, and *-1C*, have been reported, with PDE1A and -1C expressed in the heart (13). PDE1A hydrolyzes cGMP with greater affinity than cAMP, whereas PDE1C hydrolyzes both similarly. We previously demonstrated that treatment with a pan-PDE1 inhibitor significantly reduced isoproterenol (ISO)-induced cardiac hypertrophy and fibrosis (13, 14), but these studies were unable to delineate the contributions of individual PDE1 isozymes to this effect. Our preliminary studies indicated that PDE1C expression is increased in failing human and mouse hearts; therefore we investigated the regulation and function of PDE1C in pathological cardiac

Significance

Heart failure is the leading global cause of death; therefore developing a greater understanding of disease etiology and identifying novel therapeutic targets is critical. Here, we describe the role of the cyclic nucleotide-degrading protein phosphodiesterase 1C (PDE1C) in the context of pathological cardiac remodeling. In cardiac myocytes, we found that PDE1C regulates both cyclic AMP- and cyclic GMP-mediated signaling pathways under different conditions. In both isolated cells and mice we found that inhibition of PDE1C could potentiate protective signaling and prevent the development of many aspects of heart failure, potentially by signaling through multiple cell types. PDE1 inhibition therefore may represent a viable therapeutic strategy for treatment of heart failure.
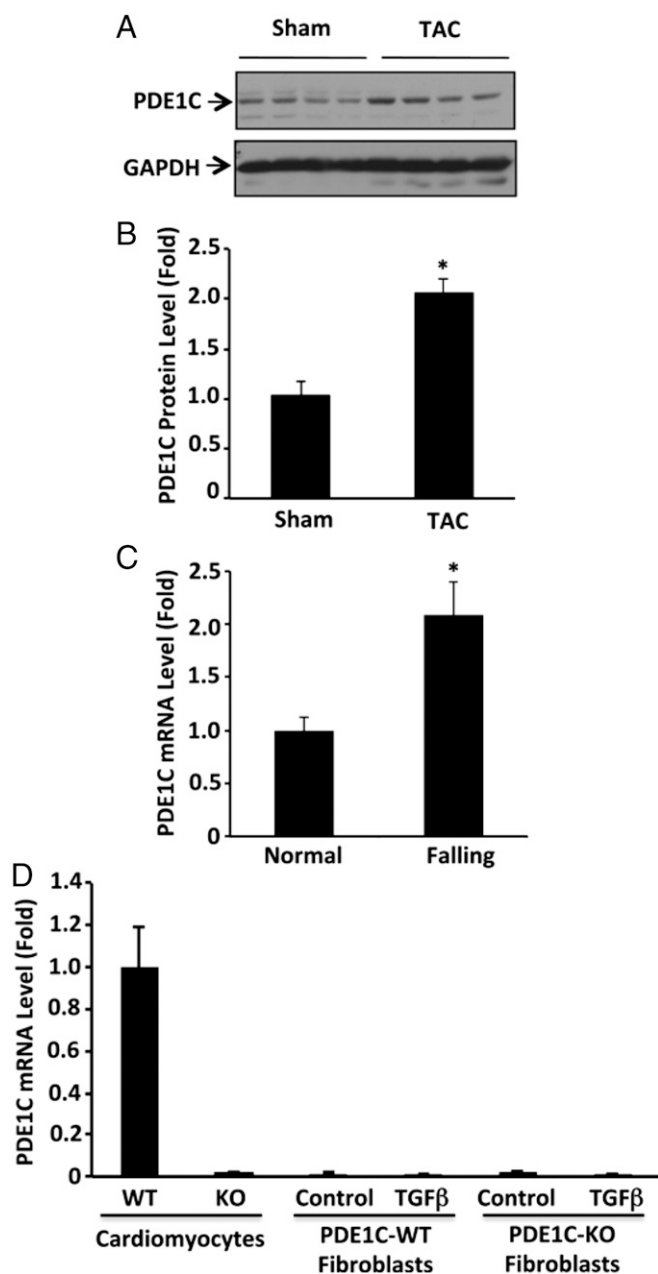
Fig. 1. PDE1C expression is increased in failing hearts. (A) Representative Western blots showing PDE1C expression in hearts from mice 8 wk after TAC or a sham operation. GAPDH is used as a control. (B) Densitometric quantification of Western blots of PDE1C normalized to GAPDH protein; $n = 12$ for sham-operated hearts; $n = 17$ for TAC hearts. (C) PDE1C mRNA levels as assessed by qPCR in heart tissue from human healthy donors or from failing hearts, normalized to GAPDH; $n = 23$ for tissue from healthy hearts; $n = 27$ for tissue from failing hearts. *$P < 0.05$ vs. sham. (D) PDE1C mRNA levels as assessed by qPCR in cardiac myocytes and cardiac fibroblasts isolated from PDE1C-WT and -KO mice; $n = 4$ for cardiac myocytes; $n = 3$ for fibroblasts.

remodeling through a combination of in vitro and in vivo approaches. Using PDE1C-deficient mice, we determined that PDE1C plays a causative role in cardiac remodeling and dysfunction induced by chronic pressure overload. In vitro, PDE1C inhibition or depletion regulated both cardiac myocyte apoptosis and hypertrophy in response to multiple stimuli in a PKA-dependent manner. Our findings may have significant therapeutic impact and could lead to the development of novel treatment strategies, such as the use of PDE1

inhibitors in treating pathological cardiac remodeling and dysfunction.

Results

PDE1C Expression in Failing Hearts. Initially, using quantitative RT-PCR (qRT-PCR), we performed discovery screening for all PDE isoforms in mouse hearts subjected to sham operation or to transverse aortic constriction (TAC) and found that PDE1C expression was increased in TAC hearts. Therefore, we sought to investigate the regulation and function of PDE1C in cardiac disease further. We first confirmed up-regulation of PDE1C protein in mouse TAC hearts relative to sham-operated hearts (Fig. 1 A and B). We also found that PDE1C mRNA is increased in tissue from failing human hearts compared with heart tissue from healthy donors (Fig. 1C). In line with our findings, a recent RNA-sequencing study of samples from failing human hearts reported increased PDE1C expression in both ischemic heart disease and dilated cardiomyopathy (15).

Expression of PDE1C in Cardiac Cells. To determine the cardiac cell types expressing PDE1C, we analyzed PDE1C expression in isolated adult cardiac myocytes and fibroblasts through qPCR. As shown in Fig. 1D, we found that PDE1C is highly expressed in cardiac myocytes but has negligible expression in fibroblasts.

Role of PDE1C in Cardiac Myocyte Death and Apoptosis in Vitro. To investigate whether PDE1C plays a direct role in regulating cardiac myocyte death, we isolated cardiac myocytes from PDE1C-WT and -KO mice and induced cell death with angiotensin II (Ang II) or ISO treatment. Cell death was detected by Trypan blue staining (Fig. 2A), apoptosis was measured by TUNEL staining (Fig. 2C), and cytotoxicity was evaluated further by lactate dehydrogenase (LDH) colorimetric assay (Fig. 2E). Ang II treatment induced a significant increase in Trypan blue-positive cells in PDE1C-WT myocytes but largely failed to do so in PDE1C-KO myocytes (Fig. 2B). In addition, PDE1 inhibition via IC86340 (a pan-PDE1 inhibitor) almost completely blocked Ang II-induced cell death in PDE1C-WT myocytes but had no further effect on PDE1C-KO myocytes (Fig. 2B), suggesting that the protective effect of IC86340 is achieved primarily by inhibiting PDE1C in cardiac myocytes. Similarly, Ang II-induced apoptosis seen in PDE1C-WT cells was diminished in PDE1C-KO myocytes; IC86340 treatment again was protective only in PDE1C-WT myocytes (Fig. 2D). In line with the results produced by cell biology-based methods, the LDH release assay demonstrated that Ang II induced significant LDH release in PDE1C-WT cardiac myocytes and that this release was blocked by PDE1 inhibition or PDE1C deficiency (Fig. 2E). These findings also confirmed that Trypan blue staining is a valid method for assessing cell death in cardiac myocytes in vitro; we therefore used it for the majority of further experiments investigating cell death. In contrast to PDE1C deficiency, ectopic expression of PDE1C1 through adenoviral vectors in PDE1C-KO myocytes resensitized them to Ang II-stimulated cell death, which could be blocked by IC86340 (Fig. 2F).

Furthermore, ISO-induced cell death also was inhibited dose-dependently by IC86340 (Fig. S1A), and although ISO significantly increased cell death in PDE1C-WT cardiac myocytes, it failed to do so in IC86340-treated cells or in PDE1C-KO myocytes (Fig. S1B). These findings suggest that PDE1 plays a critical role in regulating myocyte death/apoptosis and that PDE1C is the major PDE1 isoform responsible for this effect.

Because PDE1C hydrolyzes both cAMP and cGMP with high affinity in cell-free systems (16), we examined the effect of inhibiting the potential downstream targets, cAMP-dependent protein kinase (PKA, a downstream cAMP effector) and cGMP-dependent protein kinase (PKG, a downstream cGMP effector), on the protective effect of PDE1C inhibition. Although the PKA inhibitor PKI largely abolished the protective effect of IC86340 on Ang II-induced cell death, the peptide PKG inhibitor DT-2 (Fig. 3A) and the cGMP analog PKG inhibitor Rp-8-Br-PET-cGMPs (Fig. S2A) failed to do so. To confirm that PKI did not induce cell death independently of Ang II, we also treated PDE1C-WT cardiac
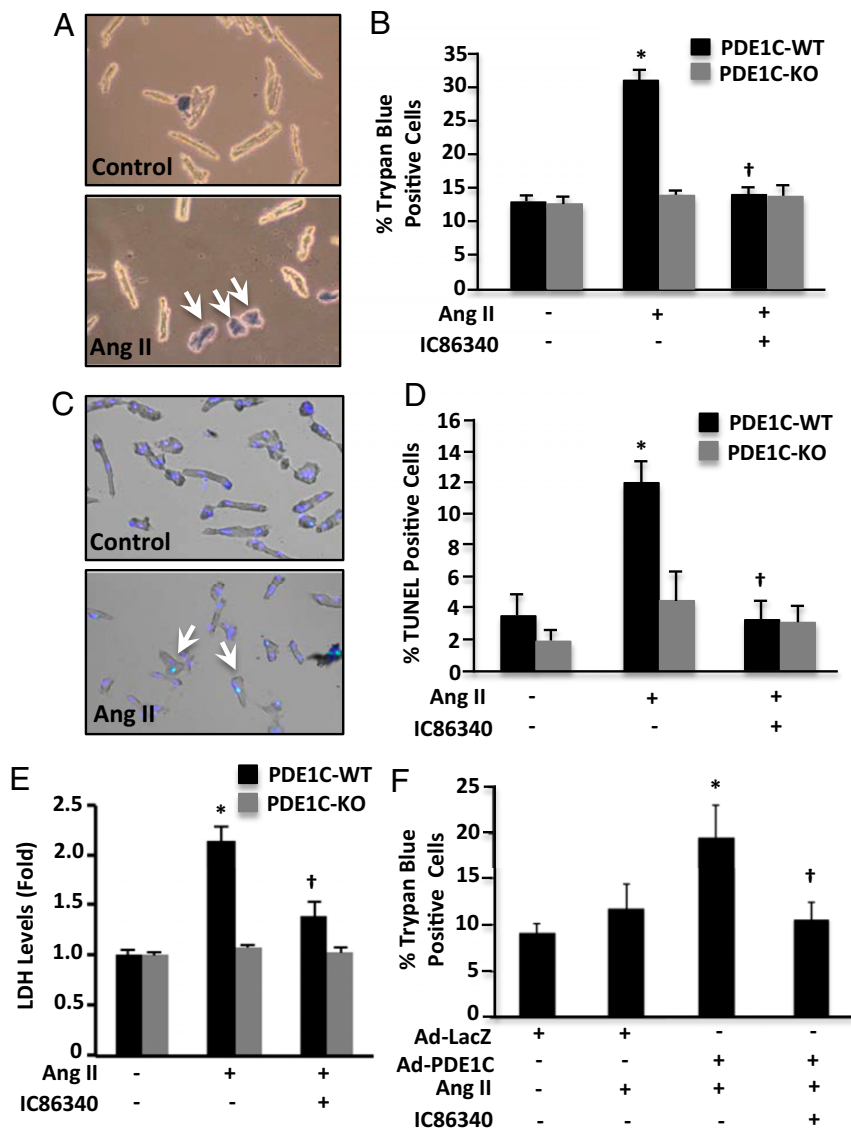
Fig. 2. Role of PDE1C in cardiac myocyte death. (A–D) Cardiac myocytes were isolated from PDE1C-WT or -KO mice, and cell death was stimulated by 200 nM Ang II in the presence of vehicle or IC86340 (15 μM) as indicated. (A) Trypan blue staining after 24 h. White arrows point to Trypan blue-positive myocytes. (B) Quantification of Trypan blue-positive cells. (C) TUNEL staining after 48 h. Nuclei were stained with DAPI (blue). White arrows point to TUNEL-positive apoptotic cells. (D) Quantification of TUNEL-positive nuclei. (E) LDH release assay of PDE1C-WT and -KO cardiac myocytes after treatment for 24 h with Ang II and IC86340 as indicated. (F) Trypan blue staining of PDE1C-KO myocytes transduced with adenovirus expressing LacZ or PDE1C1 for 24 h and stimulated with Ang II for 24 h in the presence of vehicle or IC86340. *$P < 0.05$ vs. control (B, D, and E) or vs. Ad-LacZ (F); †$P < 0.05$ vs. Ang II (B, D, and E) or vs. Ad-PDE1C/Ang II (F). $n = 3$–6 per study.

myocytes with PKI alone and found that it failed to induce appreciable cell death (Fig. S2B).

We next investigated the role of PDE1C in regulating cAMP. Because PDE1C is a Ca^{2+}/calmodulin (CaM)-stimulated PDE (16), we speculated that Ang II treatment could increase its activity in cardiac myocytes. We found that in PDE1C-WT myocytes Ang II induced a reduction in cAMP, which was abolished by inhibiting PDE1 with IC86340 (Fig. 3B). However, Ang II failed to reduce cAMP in PDE1C-KO myocytes (Fig. 3C). These results suggest the involvement of a cAMP-dependent mechanism in PDE1C-mediated regulation of myocyte death.

It is known that stimulation of certain G$_s$-coupled/cAMP-elevating receptors, such as adenosine type 2 receptors (A$_2$R) (17) and glucagon-like peptide 1 receptors (GLP1R) (18), leads to protection against cardiac myocyte death. Several reports have indicated that PI3K/AKT is critical in mediating these protective effects (18–20). Therefore, we examined the role of PI3K/AKT in PDE1C-mediated myocyte protection. Interestingly, we found that pharmacological inhibition of either PI3K with LY294002 or of AKT with MK2206 blocked the protective effects of PDE1 inhibition as assessed by Trypan blue staining (Fig. 3 D and E) and LDH release (Fig. S2C). This finding suggests that PI3K/AKT signaling plays a critical role in PDE1C-mediated regulation of cell death.

The Role of PDE1C in Cardiac Myocyte Hypertrophy in Vitro. We next examined whether PDE1C directly regulates cardiac myocyte hypertrophy. Isolated adult mouse cardiac myocytes from PDE1C-WT and -KO mice were stimulated with Ang II or ISO for 72 h in the presence of blebbistatin (a myosin II inhibitor) to block myocyte contraction and to extend their survival during culture (21). Myocyte hypertrophy was assessed by measuring the average cell area. In PDE1C-WT cardiac myocytes, both Ang II and ISO treatment stimulated significant cardiac myocyte hypertrophy (Fig. 4A and Fig. S3A). However, in PDE1C-KO cells, Ang II failed to stimulate hypertrophy (Fig. 4A), but ISO-induced hypertrophy was partially attenuated as assessed by an increase in cell area (Fig. S3A). Additionally, we assessed the expression of the hypertrophic marker atrial natriuretic peptide (ANP) and found that Ang II induced significant ANP elevation in PDE1C-WT cardiac myocytes but failed to do so in the PDE1C-KO cells (Fig. 4B).

We next determined the role of PKA and PKG in the antihypertrophic effects of PDE1C deficiency with PKA or PKG inhibitors. Consistent with PDE1C's role in regulating cell death, we found that inhibition of PKA by PKI attenuated the antihypertrophic effect of PDE1C deficiency in response to Ang II treatment (Fig. 4C). Interestingly, PKG inhibition with DT-2 induced hypertrophy under basal conditions in PDE1C-KO cardiac

Fig. 3. Role of PKA/PKG and PI3K/AKT signaling in PDE1C-mediated regulation of cardiac myocyte death. (*A*) Quantification of Trypan blue staining on myocytes pretreated with the PKG inhibitor DT-2 (1 μM) or the PKA inhibitor PKI (5 μM) in addition to IC86340 (15 μM) and Ang II, as indicated, for 24 h. (*B* and *C*) cAMP levels in PDE1C-WT (*B*) or PDE1C-KO (*C*) cardiac myocytes pretreated with IC86340 and stimulated with Ang II for 15 min as indicated. (*D*) WT cardiac myocytes were pretreated with 15 μM IC86340, with the PI3K inhibitor LY294002 (10 nM), or with both, as indicated, followed by treatment with 200 nM Ang II for 24 h to induce cell death. (*E*) WT cardiac myocytes were pretreated with 15 μM IC86340, with the AKT inhibitor MK-2206 (500 nM), or with both, as indicated. *$P < 0.05$ vs. control; †$P < 0.05$ vs. Ang II; #$P < 0.05$ vs. Ang II/IC86340; $n = 3$ per experiment.

Fig. 4. The role of PDE1C in cardiac myocyte hypertrophy in vitro. (*A*) Cardiac myocytes were isolated from PDE1C-WT or -KO mice and stimulated with Ang II (100 nM) for 72 h. Cells then were fixed and photographed under a microscope. The cell area was averaged from $n > 1,900$ cells from five isolations. (*B*) ANP mRNA levels in PDE1C-WT and -KO cardiomyocytes treated with Ang II for 72 h as indicated; $n = 3$. (*C*) Cardiac myocytes were isolated from PDE1C-KO mice and were pretreated with the PKG inhibitor DT-2 (1 μM) or the PKA inhibitor PKI (5 μM), followed by Ang II treatment for 72 h as indicated. Cardiac myocyte areas were quantified from $n > 1,000$ myocytes from three isolations. *$P < 0.05$ vs. control; †$P < 0.05$ vs. + Ang II.

myocytes (Fig. 4*C*). However, Ang II treatment in combination with DT-2 failed to induce any further cell hypertrophy compared with DT-2 alone (Fig. 4*C*). To determine whether this effect was specific to PDE1C-KO cardiac myocytes, we also treated WT cardiac myocytes with DT-2 and PKI and found that neither treatment alone had any significant effect on cell hypertrophy (Fig. S3*B*). These results suggest PKA mediates the inhibitory effects of PDE1C deficiency on Ang II-stimulated myocyte hypertrophy, although it is not yet clear how DT-2 treatment alone induces myocyte hypertrophy specifically in PDE1C-KO myocytes.

PDE1C Deficiency Ameliorates TAC-Induced Cardiac Dysfunction in Vivo. To investigate whether PDE1C plays a causative role in pathological cardiac remodeling in vivo, we subjected PDE1C-WT and -KO mice to TAC or to a sham operation as control. PDE1C-KO mice are physiologically normal aside from a defect in sensitivity and adaptation in olfactory neurons (22). We did not observe any significant difference in heart rate (Table 1) or blood pressure between PDE1C-WT and -KO mice, as is consistent with our finding that PDE1C is not expressed in normal vessels (23). Cardiac function was monitored by echocardiography throughout the study (Fig. 5*A*). As expected, PDE1C-WT mice experienced a time-dependent loss of contractile function, as assessed by percentage of fractional shortening (FS) and ejection fraction (EF), with progression into heart failure (FS <20%) usually occurring within 8–10 wk after surgery (Fig. 5 *B* and *C* and Table 1). However, this loss of cardiac function was markedly attenuated in PDE1C-KO mice. Furthermore, TAC-induced increases in left ventricular (LV) diameter at systole (LVID, s) and diastole (LVID, d), indicators of chamber dilation, were also drastically attenuated in PDE1C-KO mice relative to PDE1C-WT (Fig. 5 *D* and *E*).

PDE1C Deficiency Attenuates TAC-Induced Cardiac Structural Remodeling in Vivo. We next evaluated morphological and structural changes in TAC-treated hearts, including global heart size (Fig. 6A) and the ratio of ventricular weight to tibia length (Fig. 6B) or body weight (Table 1). TAC-induced increases in heart size and weight were markedly reduced in PDE1C-KO mice. The ratio of LV mass to body weight, as calculated by echocardiography, was also significantly reduced in PDE1C-KO mice (Fig. 6C). Furthermore, cardiac expression of the prohypertrophic markers ANP, B-type natriuretic peptide (BNP), and β-myosin heavy chain (β-MHC) were induced by TAC in PDE1C-WT mice but were significantly reduced in PDE1C-KO TAC mice (Fig. 6 D and F). Although we observed a considerable reduction in global cardiac hypertrophy in PDE1C-KO TAC compared with PDE1C-WT TAC mice, we did not see a reduction in either anterior or posterior LV wall thickness in PDE1C-KO mice (Table 1). This difference likely can be explained by the considerable LV dilation observed in PDE1C-WT TAC mice. Although wall thickness was similar in the two genotypes, PDE1C-WT TAC hearts had a much greater internal ventricular diameter and volume; therefore their overall heart mass was drastically increased.

We further analyzed myocyte hypertrophy specifically in vivo by assessing myocardial cross-sectional area (CSA) using wheat germ agglutinin (WGA) staining (Fig. 7A). TAC induced a significant increase in CSA in PDE1C-WT hearts, but this effect was markedly reduced in PDE1C-KO hearts (Fig. 7B). We also assessed cardiac fibrosis using Masson's trichrome staining (Fig. 7C). Although TAC-induced interstitial fibrosis was significantly reduced in PDE1C-KO hearts compared with PDE1C-WT hearts, perivascular fibrosis was induced similarly in the two genotypes (Fig. 7D), suggesting that PDE1C regulates interstitial fibrosis specifically. Furthermore, myocyte apoptosis was evaluated by double staining for the myocyte marker α-actinin and TUNEL-positive nuclei (Fig. 7E). TAC-treated PDE1C-WT hearts displayed a significant increase in cardiac myocyte apoptosis (marked with arrows in Fig. 7E) relative to sham-operated hearts, but, again, this effect was largely suppressed in PDE1C-KO hearts (Fig. 7F). To determine whether compensatory up-regulation of other PDEs occurred in response to PDE1C depletion, we also examined the

Fig. 5. Genetic deletion of PDE1C attenuates TAC-induced cardiac dysfunction. PDE1C-WT and PDE1C-KO mice at 8–12 wk of age were subjected to TAC or to a sham operation. Cardiac function was monitored via echocardiography at baseline and at 2, 4, 8, and 10 wk after surgery. (A) Representative M-mode echocardiographic images of each study group. (B–E) Summaries of the echocardiographic data of each group. *$P < 0.05$ WT TAC vs. WT sham; †$P < 0.05$; KO TAC vs. WT TAC. Animal numbers: PDE1C-WT sham: $n = 6$; PDE1C-WT TAC: $n = 10$; PDE1C-KO sham: $n = 5$; and PDE1C-KO-TAC: $n = 10$.

Table 1. Cardiac function of PDE1C-WT and -KO mice

Parameters	WT sham operated, $n = 6$		WT TAC, $n = 10$		PDE1C-KO sham operated, $n = 5$		PDE1C- KO TAC, $n = 10$	
	Baseline	10 wk post surgery	Baseline	10 wk post surgery	Baseline	10 wk post surgery	Baseline	10 wk post surgery
EF (%)	81.50 ± 0.28	80.16 ± 0.65	80.95 ± 0.27	30.97 ± 4.56*	80.44 ± 0.99	78.35 ± 0.63	80.32 ± 0.66	69.33 ± 4.73[†]
LVAW,d (mm)	0.81 ± 0.04	0.75 ± 0.03	0.77 ± 0.02	1.04 ± 0.07*	0.86 ± 0.03	0.90 ± 0.05	0.81 ± 0.02	1.21 ± 0.05[†]
LVAW,s (mm)	1.20 ± 0.05	1.24 ± 0.01	1.19 ± 0.02	1.25 ± 0.08	1.25 ± 0.04	1.30 ± 0.03	1.22 ± 0.03	1.60 ± 0.06[†]
LVPW,d (mm)	0.67 ± 0.02	0.64 ± 0.03	0.69 ± 0.02	1.06 ± 0.06*	0.68 ± 0.03	0.76 ± 0.05	0.69 ± 0.02	0.99 ± 0.06
LVPW,s (mm)	1.05 ± 0.03	1.14 ± 0.02	1.07 ± 0.03	1.13 ± 0.07	1.07 ± 0.05	1.08 ± 0.03	1.05 ± 0.02	1.28 ± 0.07
LVV,d (μL)	38.2 ± 1.69	55.46 ± 4.02	41.38 ± 1.77	121.44 ± 17.78*	42.89 ± 1.48	48.43 ± 5.18	37.65 ± 1.88	48.88 ± 5.83[†]
LVV,s (μL)	7.07 ± 0.33	11.08 ± 1.07	7.90 ± 0.39	90.11 ± 17.21*	8.40 ± 0.54	10.56 ± 1.29	7.48 ± 0.54	17.3 ± 5.18[†]
Body weight (g)	24.37 ± 0.98	27.98 ± 01.04	25.45 ± 0.56	27.19 ± 0.86	27.06 ± 0.56	30.62 ± 0.78	24.05 ± 0.53	27.77 ± 0.72
Heart rate (beats/min)	551.79 ± 0.79	597.24 ± 7.05	551.27 ± 7.53	543.16 ± 12.54*	546.83 ± 6.12	565.71 ± 7.38	553.10 ± 10.45	549.49 ± 7.60

LVAW, d/s: left ventricular anterior wall diameter at diastole/systole; LVPW, d/s: left ventricular posterior wall diameter at diastole/systole; LVV, d/s: left ventricular volume at diastole/systole. Values are expressed as mean ± SEM.
*$P < 0.05$ vs. WT/sham.
[†]$P < 0.05$ vs. WT/TAC.

expression of a number of other cAMP-hydrolyzing PDEs previously reported in the heart, including PDE1A, -2A, -3A, -3B, -4D, and -8A (Fig. S4A). We did not observe any significant changes in the expression of other PDE isozymes between PDE1C-WT and -KO hearts. We also assessed PDE activities in PDE1C-WT and -KO hearts. As expected, in WT heart, PDE1 cAMP-hydrolyzing activity was much higher in the presence of Ca^{2+}/CaM than in the presence of EGTA, and this higher activity was largely suppressed in PDE1C-KO heart. This result indicates that PDE1C represents the major cardiac cAMP-hydrolyzing activity when Ca^{2+} signaling is stimulated. Although most PDE activities were similar in the two genotypes, we observed a modest increase in PDE4 activity in PDE1C-KO hearts (Fig. S4B).

The Role of Myocyte PDE1C in the Regulation of Fibroblast Activation.
Although we failed to detect PDE1C in cardiac fibroblasts, because we observed reduced cardiac fibrosis in PDE1C-KO hearts, we examined the effect of PDE1C deficiency on TGF-β–stimulated cardiac fibroblast activation by assessing the expression of smooth muscle α-actin (α-SMA), a marker of fibroblast-to-myofibroblast conversion. We found that TGF-β treatment stimulated α-SMA expression similarly in PDE1C-WT and -KO fibroblasts (Fig. 8 A and B), further indicating that PDE1C does not function directly in cardiac fibroblasts. This result is in line with the lack of PDE1C expression in fibroblasts and myofibroblasts (Fig. 1D). Because crosstalk between myocytes and fibroblasts has been shown to be important in the development of cardiac fibrosis (24), we hypothesized that the antifibrotic effect of PDE1C deficiency seen in vivo (Fig. 7D) could be a secondary effect of PDE1C depletion in myocytes. Potentially, such an effect could be mediated by a cardiac myocyte-derived secreted factor. To test this hypothesis, we collected conditioned medium from PDE1C-WT and -KO cardiac myocyte cultures and tested whether treatment of fibroblasts with this medium could modulate their activation by TGF-β. Interestingly, TGF-β stimulation elicited a robust increase in α-SMA expression in cardiac fibroblasts treated with medium from PDE1C-WT myocytes but resulted in significantly lower α-SMA expression in fibroblasts treated with medium from PDE1C-KO myocytes (Fig. 8C). Therefore it appears likely that a cardiac myocyte-derived factor is capable of mediating fibroblast activation, perhaps accounting for the antifibrotic effects of PDE1C deficiency in vivo.

Discussion
In this study, we used genetic and pharmacological approaches both in vitro and in vivo to explore the role and mechanism of PDE1C in pathological cardiac remodeling and dysfunction. We found that PDE1C deficiency or inhibition attenuates cardiac remodeling and dysfunction by antagonizing cardiac myocyte hypertrophy and death as well as cardiac fibroblast activation (Fig. 8D). This study includes the following major findings: (i) we showed that PDE1C expression is up-regulated in failing animal and human hearts and that PDE1C-deficient mice subjected to TAC displayed attenuated myocardial hypertrophy, myocardial death, chamber dilation, and contractile dysfunction. This finding suggests that PDE1C plays a detrimental role in the development of heart failure induced by chronic pressure overload. (ii) In cardiac myocytes, PDE1C negatively regulates protective cAMP/PKA signaling that antagonizes myocyte death as well as hypertrophic growth. Activation of PI3K/AKT appears to be necessary for mediating the protective effects of PDE1C depletion on cell death. (iii) We found that although PDE1C is expressed exclusively in cardiac myocytes and not in fibroblasts, PDE1C in myocytes likely regulates myocyte production of secreted factor(s) that are important for fibroblast activation and fibrosis. Thus, PDE1C may represent a compelling therapeutic target, because inhibition of this enzyme may prevent diverse aspects of pathological cardiac remodeling in multiple cell types. In addition, we have shown previously that the PDE1A isoform inhibition attenuates cardiac myocyte hypertrophy (13) and fibroblast activation (14) largely through a cGMP-dependent mechanism. Thus, our previous and current findings may have considerable therapeutic impact, because they may lead to the development of novel therapeutic strategies using PDE1 inhibitors to combat pathological cardiac remodeling and dysfunction. Currently, a pan-PDE1 inhibitor is under development for treating schizophrenia by targeting the PDE1B isozyme in the brain (25), suggesting the potential safety of using PDE1 inhibitors as therapeutic agents. Therefore, the therapeutic effects of PDE1 inhibitors in cardiac remodeling and failure deserve further investigation in preclinical animal models.

Increasing evidence indicates that in cardiac myocytes multiple spatially and functionally distinct cAMP/PKA-signaling modules are activated through different G protein-coupled receptors (GPCRs) and regulated by different PDEs. For example, chronic stimulation of β-AR, particularly β1-AR, activates cAMP/PKA signaling, which promotes myocyte death and hypertrophy and cardiac remodeling (3, 4). In contrast, activating cAMP/PKA signaling by stimulating A_2R appears to be cardioprotective. For example, A_2R activation attenuated TAC-induced cardiac dysfunction (26) and prevented pathological remodeling in response to myocardial infarction (27). A_2R activation also is necessary for the cardioprotective effects of ischemic postconditioning (20). Stimulating

GLP1R and cAMP/PKA signaling also can prevent cardiac myocyte death (18, 28). PDE3 appears to be important in regulating β-AR–stimulated cAMP-signaling modules. Chronic inhibition of PDE3A function triggered cardiac myocyte apoptosis (4, 29), whereas myocardial overexpression of PDE3A1 prevented cardiac myocyte apoptosis and ischemia/reperfusion-induced myocardial injury (30). In this study we found that PDE1C deficiency and inhibition increased cAMP and exhibited antiapoptotic and antihypertrophic effects through a PKA-dependent mechanism. This finding suggests that PDE1C may couple specifically to a protective cAMP-signaling module in cardiac myocytes. Thus, it would be reasonable to determine in the future whether PDE1C modulates A2R- or GLP1R-mediated cAMP signaling modules or other cAMP-mediated cardiac-protective pathways. We found that PI3K or AKT inhibition blocked PDE1's protective inhibition of cardiac myocytes' death (Fig. 3 D and E and Fig. S2C), potentially suggesting the involvement of PI3K/AKT signaling. Although the relationship between PKA and PI3K/AKT in cardiomyocytes is not well established, PKA-mediated phosphorylation of the PI3K regulatory subunit p85α (p85α^PI3K) and subsequent activation of AKT has been reported to be responsible for the prosurvival effects of cAMP in FRTL-5 thyroid (31) and MCF-7 breast cancer cells (32). Therefore, it is possible that cAMP/PKA could modulate PI3K/AKT signaling directly in cardiac myocytes as well; this possibility deserves further characterization in the future.

Genetic compensation may occur because of chronic depletion of PDE1C. To address this issue in PDE1C-deficient mice, we analyzed the levels of cardiac expression and enzyme activity for PDE1A and a number of cAMP-hydrolyzing PDEs that have been reported in the heart. We did not detect a significant change in gene expression and activity for most of these PDEs, aside from a modest increase in PDE4 activity (Fig. S4B). Increasing PDE4 activity potentially could be cardiac protective, because loss of PDE4B results in tachycardia and arrhythmias (33) and because loss of PDE4D function promotes cardiac arrhythmogenesis and heart failure (9). However, we previously found that PDE4 inhibitors did not have significant effects on cardiac myocyte apoptosis (4, 29). Therefore it is unlikely that the up-regulation of PDE4 activity seen in PDE1C-KO hearts contributes to the antiapoptotic effect of PDE1C deficiency. It is not surprising that depletion of PDE1C did not drastically alter the expression and activity of other PDE isozymes, because different PDE isozymes likely regulate multiple, discretely compartmentalized cyclic nucleotide-signaling modules. Another potential concern of this study is that the noncardiac effects of PDE1C depletion might modulate cardiac remodeling indirectly. Although we cannot rule out this possibility when using global PDE1C-KO mice, our findings obtained using isolated cardiac myocytes from PDE1C-WT and -KO mice strongly support the notion that PDE1C functions directly in cardiac myocytes. Nevertheless, the generation of mice with cardiac myocyte-specific depletion of PDE1C in the future will be helpful.
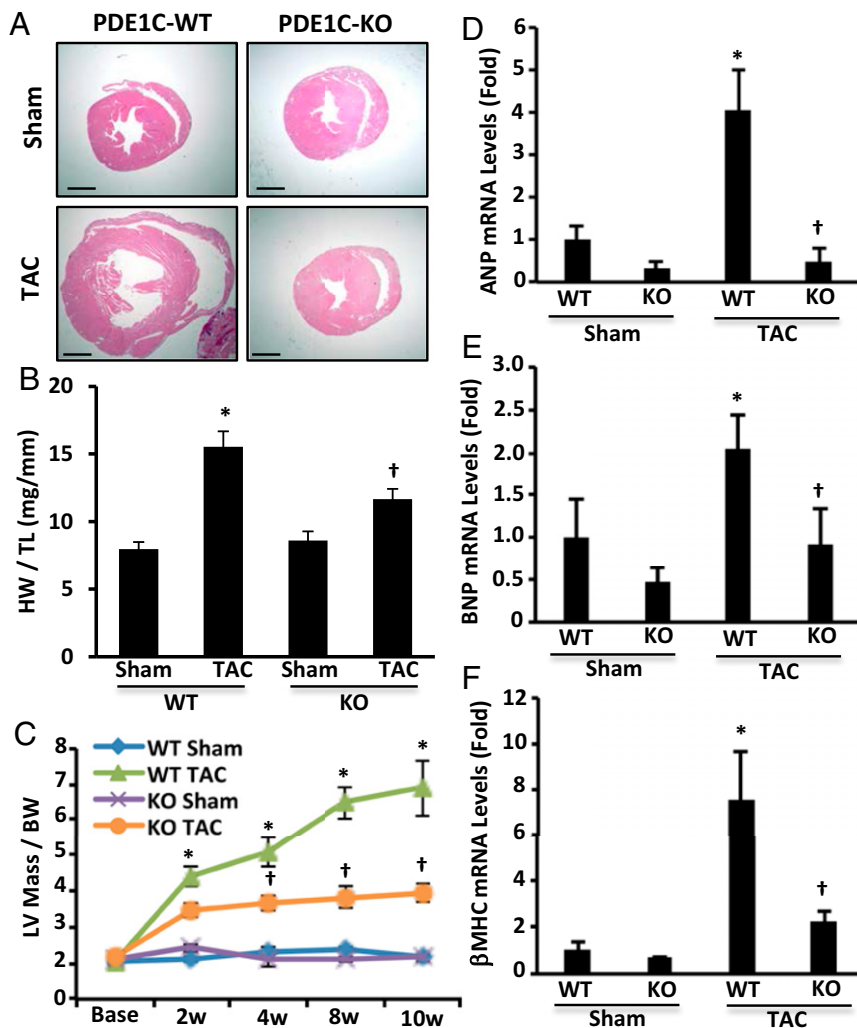

Fig. 6. PDE1C deficiency attenuates TAC-induced cardiac hypertrophy. (A) Representative H&E-stained heart cross-sections. (Scale bars: 1,000 μm.) (B) Heart weight (HW)-to-tibia length (TL) ratios in sham- and TAC-operated mice. (C) Ratio of LV mass, as assessed by echocardiography, to body weight throughout the duration of TAC studies. (D–F) ANP (D), BNP (E), and β-MHC (F) levels in the indicated ventricular samples assessed by qPCR and normalized to GAPDH. *P < 0.05 vs. PDE1C-WT sham-operated mice; †P < 0.05 vs. WT TAC-treated mice. Animal numbers: PDE1C-WT sham-operated: n = 6; PDE1C-WT TAC: n = 10; PDE1C-KO sham-operated: n = 5; and PDE1C-KO-TAC: n = 10.

Although PDE1C hydrolyzes both cAMP and cGMP with high affinity in cell-free conditions (16), most cellular studies to date have shown that PDE1C regulates cAMP signaling primarily in cells such as proliferating vascular smooth muscle cells (23, 34) and pancreatic B cells (35). In this study we also demonstrated that PDE1C regulates cAMP levels, particularly Ang II-mediated suppression of cAMP (Fig. 3 B and C), in cardiac myocytes. This finding suggests that Ang II activates PDE1C, likely by elevating Ca^{2+}, given that PDE1C is a Ca^{2+}/CaM-stimulated PDE. Although the source of Ca^{2+}-activating PDE1C is not established, possible candidates are the transient receptor potential canonical (TRPC) channels. These nonselective Ca^{2+} channels play an established, maladaptive role in pathological cardiac remodeling (36), and

TRPC3 and TRPC6 can become activated in response to Ang II signaling via DAG production in cardiac myocytes (37) and in other cell types (38). Potentially, one of the mechanisms by which TRPC channel activation worsens pathological remodeling could be via PDE1C activation and the suppression of protective cAMP signaling, a notion that deserves future investigation. The role of PDE1C in cGMP signaling still is not clear. Surprisingly, in this study we observed a significant increased basal myocyte area in response to treatment with the PKG inhibitor DT-2 alone in PDE1C-KO, but not in PDE1C-WT, myocytes (Fig. 4C and Fig. S3B). One possible explanation is that chronic activation of PKG signaling caused by PDE1C depletion leads to compensatory over-activation of prohypertrophic signaling, which often is antagonized
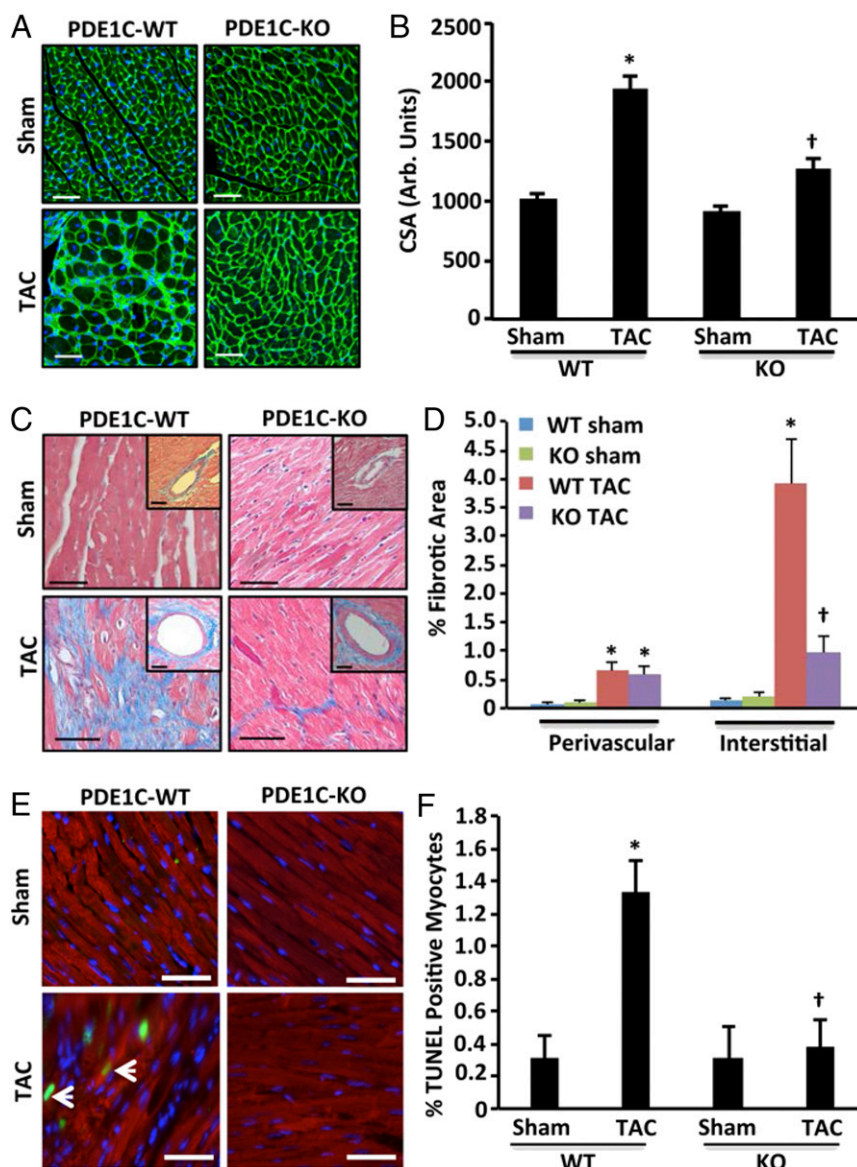
Fig. 7. Genetic deletion of PDE1C attenuates TAC-induced cardiac structural remodeling. PDE1C-WT and PDE1C-KO mice at 8–12 wk of age were subjected to TAC for 10 wk or to a sham operation. (A) Representative images of WGA staining in mouse hearts after the sham operation or TAC. (B) Cardiac myocyte hypertrophy was quantified by assessing cross-sectional cell-surface areas from WGA staining. At least 300 myocytes were quantified per heart. (C) Representative images of heart sections stained with Masson's trichrome. Large images show interstitial fibrosis; Insets show perivascular fibrosis. Blue staining shows fibrotic areas. (D) Quantification of cardiac fibrosis. (E) Representative images of cardiac myocyte apoptosis in hearts subjected to the sham operation or TAC. Green indicates TUNEL-positive (apoptotic) nuclei, red indicates α-actinin (myocyte) staining, and blue represents DAPI staining for nuclei. TUNEL-positive nuclei occurring in α-actinin–positive cells were considered to be apoptotic cardiac myocytes (white arrows). (F) Quantification of TUNEL-positive cardiac myocytes. (All scale bars: 50 μm.) *$P < 0.05$ vs. WT sham; †$P < 0.05$ vs. WT TAC. Animal numbers: PDE1C-WT sham: $n = 6$ in A–F; PDE1C-WT TAC: $n = 10$ in A–D, and $n = 8$ in E and F; PDE1C-KO sham: $n = 5$ in A–F; PDE1C-KO-TAC: $n = 9$ in A and B, $n = 10$ in C and D, and $n = 5$ in E and F.

by PKG signaling in PDE1C-KO myocytes. DT-2 releases PKG's inhibition of this prohypertrophic signaling and thus could induce myocyte hypertrophy. To confirm this possibility, further studies using acute PDE1C depletion/inhibition and more specific PKG blockade will be required. Many studies have reported that PKG signaling has antihypertrophic functions in cardiac myocytes (39–41); however, because of the lack of effects of cardiomyocyte PKG depletion on cardiac myocyte hypertrophy and cardiac remodeling in certain models of cardiac hypertrophy and dysfunction, this notion remains somewhat controversial (42, 43).

The precise mechanism by which PDE1C regulates cardiac fibrosis is not clear. Our finding that medium from PDE1C-KO myocytes can partially attenuate cardiac fibroblast activation may support the notion that antifibrotic paracrine signaling occurs between cardiac myocytes and fibroblasts in PDE1C-KO hearts. This notion also could account for the differences we observed between interstitial and perivascular fibrosis; because perivascular fibroblasts are localized distally to cardiac myocytes, they are less likely than interstitial fibroblasts to be significant targets of cardiac myocyte-derived paracrine signaling. Although identifying the factor(s) responsible for this antifibrotic effect remains of great interest, other explanations for our in vivo findings regarding fibrosis do exist. For example, because cardiac myocyte loss itself can lead to the replacement of dying cardiac myocytes with fibrotic tissue (44), PDE1C depletion may attenuate fibrosis simply by preventing myocyte death. Nevertheless, the exact role of PDE1C's regulation of the crosstalk between cardiac myocytes and fibroblasts and the underlying mechanism by which it does so remain to be characterized.

Materials and Methods

Further information is available in *SI Materials and Methods*.

Human Samples. Human heart tissue was obtained from the Kaufman Center for Heart Failure Tissue Bank at Cleveland Clinic, with Institutional Review Board (IRB) approval and patient consent. Failing human heart tissue was obtained from the explanted hearts of cardiac transplant recipients, and nonfailing tissue was obtained from unmatched organ donors. All tissue was procured in the operating room after cardioplegic arrest of the heart and was transported quickly to the laboratory, where it was frozen in liquid nitrogen.

Animals. Mice with global deletion of PDE1C were kindly provided by Haiqing Zhao, Johns Hopkins University, Baltimore, (22) and were backcrossed to C57BL/6 mice for at least nine generations. All animal procedures were performed in accordance with NIH and University of Rochester institutional guidelines.

TAC. TAC was performed on 8- to 12-wk-old male mice as described previously (4) with modifications. Briefly, mice were anesthetized with 1.5% (vol/vol) inhaled isofluorane and placed on mechanical ventilation. Left thoracotomy was performed, and a ligature was secured around the ascending aorta between the innominate and left carotid arteries, using 6-0 silk sutures tightened around a 27-gauge needle to maintain consistent ligature tension. Sham-operated mice were given a similar procedure, without actual ligation. To assess the quality and efficacy of surgery, the stenotic pressure gradient was assessed. Only TAC-operated mice that achieved a stenotic pressure gradient greater than 100 mmHg within 4 wk of TAC were included in the study.

Hearts were removed immediately after the TAC study, weighed, and divided. Apex and base portions were flash frozen and kept for protein and RNA extraction, respectively, and center sections were fixed with 4% (wt/vol) paraformaldehyde or methanol/acetic acid solution for histology. Myocyte cell-surface area was assessed via WGA staining (Thermo Fisher), fibrosis was assessed via Masson's trichrome staining, and apoptosis was assessed via TUNEL staining (Roche). These methods are described in greater detail in *SI Materials and Methods*.

Echocardiography. Cardiac function was monitored via echocardiography in anesthetized mice using a Vevo2100 echocardiography machine equipped with a 40-MHz frequency probe (VisualSonics). LV systolic and diastolic measurements were assessed in M-mode along the short axis of the LV.

Adult Mouse Cardiac Myocytes and Cardiac Fibroblasts. Cardiac myocytes and fibroblasts were isolated as described previously (30), with modifications. Briefly,
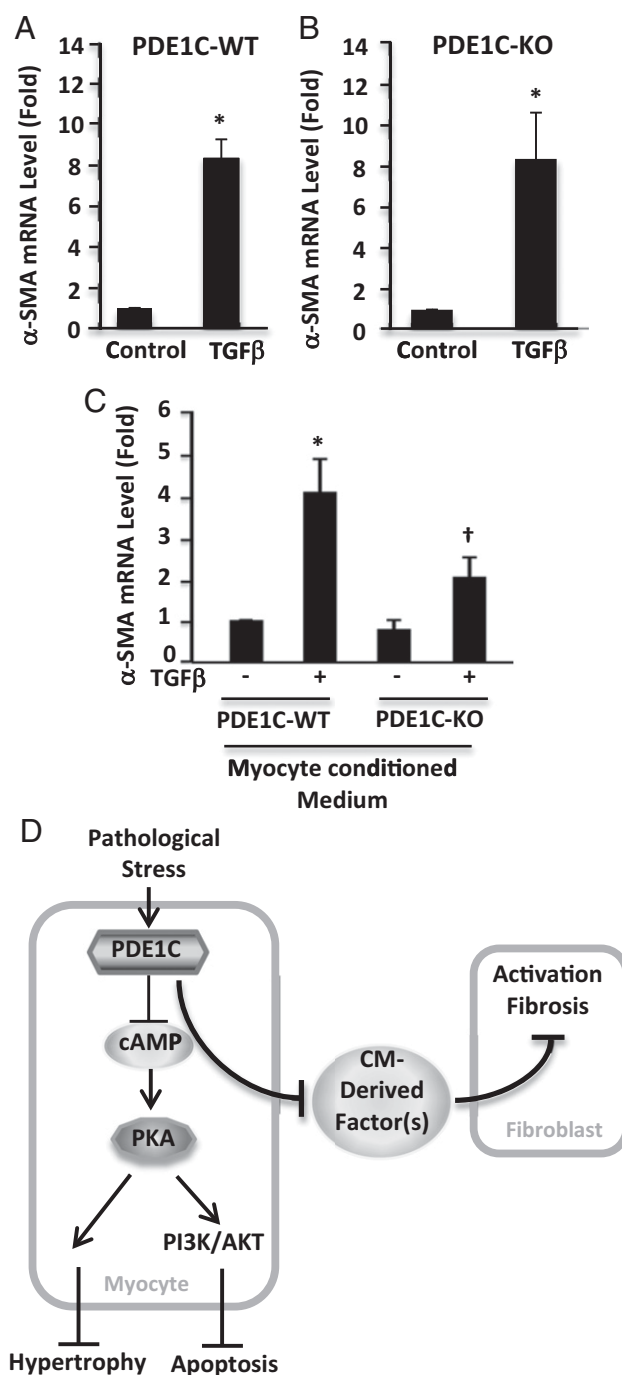

Fig. 8. The role of myocyte PDE1C in regulating cardiac fibroblast activation. (A and B) Cardiac fibroblasts were isolated from PDE1C-WT (A) or PDE1C-KO (B) mice as indicated, serum starved for 24 h, and treated with TGF-β (10 ng/mL) for 24 h to induce activation. Fibroblast activation was assessed by α-SMA mRNA levels via qPCR. (C) Conditioned medium was collected from PDE1C-WT and -KO cardiac myocytes cultured in vitro for 1 h and were used to treat WT cardiac fibroblasts. Fibroblasts then were stimulated with TGF-β for 24 h. *$P < 0.05$ vs. control; †$P < 0.05$ vs. TGF-β with WT conditioned medium, $n = 3$. (D) Proposed model.

mice were anesthetized, and the heart was removed rapidly, perfused in retrograde fashion, and digested. Cardiac myocytes were separated from fibroblasts via gravity filtration and centrifugation. Myocyte hypertrophy was assessed as described previously, with modifications (13). Myocytes were cultured with the contractility inhibitor Blebbistatin, and hypertrophy was induced via treatment with ISO (10 μM) or Ang II (100 nM) for 72 h without changing medium. Myocyte

cell death or apoptosis was induced by treatment for 24–48 h with either Ang II (200 nM) or ISO (10 μM) and was assessed via Trypan blue or TUNEL staining, respectively. Experiments were repeated a minimum of three times with two or three replicates per condition in each experiment. Fibroblasts were isolated with cardiac myocytes. Fibroblast activation, after serum-starvation for 24 h, was induced via TGF-β (10 ng/mL) for 24 h.

Statistics. All data are presented as mean ± SEM. Statistical analysis was performed using GraphPad Prism 5 (GraphPad Software). The unpaired Student's *t* test was used for comparisons of two groups, and one-way ANOVA followed by Bonferroni's post test was used for comparisons of multiple groups. *P* values <0.05 were considered significant.

1. Xu J, Kochanek KD, Murphy SL, Tejada-Vera B (2010) Deaths: Final data for 2007. *Natl Vital Stat Rep* 58(19):1–19.
2. Frey N, Olson EN (2003) Cardiac hypertrophy: The good, the bad, and the ugly. *Annu Rev Physiol* 65:45–79.
3. Communal C, Singh K, Sawyer DB, Colucci WS (1999) Opposing effects of beta(1)- and beta(2)-adrenergic receptors on cardiac myocyte apoptosis : Role of a pertussis toxin-sensitive G protein. *Circulation* 100(22):2210–2212.
4. Ding B, et al. (2005) Functional role of phosphodiesterase 3 in cardiomyocyte apoptosis: Implication in heart failure. *Circulation* 111(19):2469–2476.
5. Headrick JP, Ashton KJ, Rose'meyer RB, Peart JN (2013) Cardiovascular adenosine receptors: Expression, actions and interactions. *Pharmacol Ther* 140(1):92–111.
6. Pierre S, Eschenhagen T, Geisslinger G, Scholich K (2009) Capturing adenylyl cyclases as potential drug targets. *Nat Rev Drug Discov* 8(4):321–335.
7. Lee DI, Kass DA (2012) Phosphodiesterases and cyclic GMP regulation in heart muscle. *Physiology (Bethesda)* 27(4):248–258.
8. Rao YJ, Xi L (2009) Pivotal effects of phosphodiesterase inhibitors on myocyte contractility and viability in normal and ischemic hearts. *Acta Pharmacol Sin* 30(1):1–24.
9. Lehnart SE, et al. (2005) Phosphodiesterase 4D deficiency in the ryanodine-receptor complex promotes heart failure and arrhythmias. *Cell* 123(1):25–35.
10. Takimoto E, et al. (2005) Chronic inhibition of cyclic GMP phosphodiesterase 5A prevents and reverses cardiac hypertrophy. *Nat Med* 11(2):214–222.
11. Lee DI, et al. (2015) Phosphodiesterase 9A controls nitric-oxide-independent cGMP and hypertrophic heart disease. *Nature* 519(7544):472–476.
12. Vandeput F, et al. (2007) Cyclic nucleotide phosphodiesterase PDE1C1 in human cardiac myocytes. *J Biol Chem* 282(45):32749–32757.
13. Miller CL, et al. (2009) Role of Ca2+/calmodulin-stimulated cyclic nucleotide phosphodiesterase 1 in mediating cardiomyocyte hypertrophy. *Circ Res* 105(10):956–964.
14. Miller CL, et al. (2011) Cyclic nucleotide phosphodiesterase 1A: A key regulator of cardiac fibroblast activation and extracellular matrix remodeling in the heart. *Basic Res Cardiol* 106(6):1023–1039.
15. Liu Y, et al.; MAGNet consortium (2015) RNA-Seq identifies novel myocardial gene expression signatures of heart failure. *Genomics* 105(2):83–89.
16. Yan C, et al. (1995) Molecular cloning and characterization of a calmodulin-dependent phosphodiesterase enriched in olfactory sensory neurons. *Proc Natl Acad Sci USA* 92(21):9677–9681.
17. Jacobson KA, Gao ZG (2006) Adenosine receptors as therapeutic targets. *Nat Rev Drug Discov* 5(3):247–264.
18. Bose AK, Mocanu MM, Carr RD, Brand CL, Yellon DM (2005) Glucagon-like peptide 1 can directly protect the heart against ischemia/reperfusion injury. *Diabetes* 54(1):146–151.
19. Solenkova NV, Solodushko V, Cohen MV, Downey JM (2006) Endogenous adenosine protects preconditioned heart during early minutes of reperfusion by activating Akt. *Am J Physiol Heart Circ Physiol* 290(1):H441–H449.
20. Morrison RR, Tan XL, Ledent C, Mustafa SJ, Hofmann PA (2007) Targeted deletion of A2A adenosine receptors attenuates the protective effects of myocardial postconditioning. *Am J Physiol Heart Circ Physiol* 293(4):H2523–H2529.
21. Kabaeva Z, Zhao M, Michele DE (2008) Blebbistatin extends culture life of adult mouse cardiac myocytes and allows efficient and stable transgene expression. *Am J Physiol Heart Circ Physiol* 294(4):H1667–H1674.
22. Cygnar KD, Zhao H (2009) Phosphodiesterase 1C is dispensable for rapid response termination of olfactory sensory neurons. *Nat Neurosci* 12(4):454–462.
23. Cai Y, et al. (2015) Role of cAMP-phosphodiesterase 1C signaling in regulating growth factor receptor stability, vascular smooth muscle cell growth, migration, and neointimal hyperplasia. *Circ Res* 116(7):1120–1132.
24. Sassi Y, et al. (2014) Cardiac myocyte-secreted cAMP exerts paracrine action via adenosine receptor activation. *J Clin Invest* 124(12):5385–5397.
25. Anonymous (2011) Deal watch: Intra-Cellular Therapies and Takeda to develop PDE1 inhibitors for schizophrenia. *Nat Rev Drug Discov* 10(5):329.
26. Hamad EA, et al. (2012) Cardioprotection of controlled and cardiac-specific over-expression of A(2A)-adenosine receptor in the pressure overload. *PLoS One* 7(7):e39919.
27. Wakeno M, et al. (2006) Long-term stimulation of adenosine A2b receptors begun after myocardial infarction prevents cardiac remodeling in rats. *Circulation* 114(18):1923–1932.
28. Chang G, et al. (2013) Cardioprotective effects of exenatide against oxidative stress-induced injury. *Int J Mol Med* 32(5):1011–1020.
29. Ding B, et al. (2005) A positive feedback loop of phosphodiesterase 3 (PDE3) and inducible cAMP early repressor (ICER) leads to cardiomyocyte apoptosis. *Proc Natl Acad Sci USA* 102(41):14771–14776.
30. Oikawa M, et al. (2013) Cyclic nucleotide phosphodiesterase 3A1 protects the heart against ischemia-reperfusion injury. *J Mol Cell Cardiol* 64:11–19.
31. De Gregorio G, et al. (2007) The p85 regulatory subunit of PI3K mediates TSH-cAMP-PKA growth and survival signals. *Oncogene* 26(14):2039–2047.
32. Di Zazzo E, et al. (2014) The p85 regulatory subunit of PI3K mediates cAMP-PKA and insulin biological effects on MCF-7 cell growth and motility. *ScientificWorldJournal* 2014:565839.
33. Leroy J, et al. (2011) Phosphodiesterase 4B in the cardiac L-type Ca²⁺ channel complex regulates Ca²⁺ current and protects against ventricular arrhythmias in mice. *J Clin Invest* 121(7):2651–2661.
34. Cai Y, et al. (2011) Cyclic nucleotide phosphodiesterase 1 regulates lysosome-dependent type I collagen protein degradation in vascular smooth muscle cells. *Arterioscler Thromb Vasc Biol* 31(3):616–623.
35. Han P, Werber J, Surana M, Fleischer N, Michaeli T (1999) The calcium/calmodulin-dependent phosphodiesterase PDE1C down-regulates glucose-induced insulin secretion. *J Biol Chem* 274(32):22337–22344.
36. Wu X, Eder P, Chang B, Molkentin JD (2010) TRPC channels are necessary mediators of pathologic cardiac hypertrophy. *Proc Natl Acad Sci USA* 107(15):7000–7005.
37. Onohara N, et al. (2006) TRPC3 and TRPC6 are essential for angiotensin II-induced cardiac hypertrophy. *EMBO J* 25(22):5305–5316.
38. Ilatovskaya DV, et al. (2014) Angiotensin II has acute effects on TRPC6 channels in podocytes of freshly isolated glomeruli. *Kidney Int* 86(3):506–514.
39. Fiedler B, et al. (2002) Inhibition of calcineurin-NFAT hypertrophy signaling by cGMP-dependent protein kinase type I in cardiac myocytes. *Proc Natl Acad Sci USA* 99(17):11363–11368.
40. Frantz S, et al. (2013) Stress-dependent dilated cardiomyopathy in mice with cardiomyocyte-restricted inactivation of cyclic GMP-dependent protein kinase I. *Eur Heart J* 34(16):1233–1244.
41. Blanton RM, et al. (2012) Protein kinase g iα inhibits pressure overload-induced cardiac remodeling and is required for the cardioprotective effect of sildenafil in vivo. *J Am Heart Assoc* 1(5):e003731.
42. Lukowski R, et al. (2010) Cardiac hypertrophy is not amplified by deletion of cGMP-dependent protein kinase I in cardiomyocytes. *Proc Natl Acad Sci USA* 107(12):5646–5651.
43. Patrucco E, et al. (2014) Roles of cGMP-dependent protein kinase I (cGKI) and PDE5 in the regulation of Ang II-induced cardiac hypertrophy and fibrosis. *Proc Natl Acad Sci USA* 111(35):12925–12929.
44. Piek A, de Boer RA, Silljé HH (2016) The fibrosis-cell death axis in heart failure. *Heart Fail Rev* 21(2):199–211.
45. Murray DR, et al. (2012) β2 adrenergic activation induces the expression of IL-18 binding protein, a potent inhibitor of isoproterenol induced cardiomyocyte hypertrophy in vitro and myocardial hypertrophy in vivo. *J Mol Cell Cardiol* 52(1):206–218.
46. Beavo JA, Hardman JG, Sutherland EW (1970) Hydrolysis of cyclic guanosine and adenosine 3′,5′-monophosphates by rat and bovine tissues. *J Biol Chem* 245(21):5649–5655.
47. Kim D, et al. (2001) Upregulation of phosphodiesterase 1A1 expression is associated with the development of nitrate tolerance. *Circulation* 104(19):2338–2343.